

Effects of solvent on structural, optical and photocatalytic properties of ZnO nanostructures

Sini Kuriakose¹, Biswarup Satpati², Satyabrata Mohapatra^{1*}

¹University School of Basic and Applied Sciences, Guru Gobind Singh Indraprastha University, Dwarka, New Delhi 110078, India

²Saha Institute of Nuclear Physics, 1/AF Bidhannagar, Kolkata 700064, India

*Corresponding author. Tel: (+91) 11-25302414; E-mail: smiuac@gmail.com

Received: 20 July 2015, Revised: 22 October 2015 and Accepted: 01 November 2015

ABSTRACT

ZnO nanostructures were synthesized by a facile wet chemical method using water, ethanol and propanol as solvents. X-ray diffraction, field emission scanning electron microscopy (FESEM) and transmission electron microscopy (TEM) have been used to study the structural properties of the synthesized ZnO nanostructures, while their optical properties have been studied using UV-visible absorption spectroscopy and Raman spectroscopy. The photocatalytic activities of the as-synthesized ZnO nanostructures were evaluated by monitoring sunlight driven photocatalytic degradation of methylene blue (MB) and methyl orange (MO) dyes in water and it was observed that ZnO nanostructures prepared using propanol as a solvent exhibit highly enhanced photocatalytic activity as compared to those prepared using other solvents. The mechanism underlying the photocatalytic activity of ZnO nanostructures towards photocatalytic degradation of dyes is proposed. We attribute the highly enhanced photocatalytic activity of ZnO nanostructures prepared in propanol to the high surface area of nanosheets-like structures formed, which lead to enhanced adsorption of dye molecules resulting in efficient photocatalytic degradation of dyes upon sunlight irradiation. Copyright © 2015 VBRI Press.

Keywords: ZnO; nanostructures; photo catalysis; methylene blue; methyl orange.

Introduction

Water contamination due to hazardous water soluble organic dyes in effluents from textile and dyeing industries poses severe threat to the environment. Due to their stability these dyes cause severe ecological problems such as depleting the dissolved oxygen content of water and releasing toxic compounds that endanger the aquatic life. Photocatalytic degradation is one of the methods used for the removal of these toxic chemicals whereby the dyes are degraded through oxidation and reduction reactions in the presence of a photocatalyst [1]. Nanostructured metal oxide semiconductors have attracted great deal of interest for various electronic, optical and piezoelectric applications [2-4]. Nanostructured ZnO with wide band gap has large surface area and high UV light absorption efficiency is environment friendly [5, 6]. These properties can be used for diverse applications [7] such as UV lasers [8], field effect transistors [9], dye sensitized solar cells [10, 11], gas sensors [12] and photocatalysis [13-22]. ZnO is an n-type semiconductor having wide band gap of 3.37 eV and high exciton binding energy and has wurtzite crystal structure [23]. Nanostructured ZnO with different morphologies has been synthesized by various physical and chemical methods and is used for diverse applications [24-32]. Physical methods used include vapor-liquid-solid (VLS) growth [33], physical vapor deposition (PVD) [34], thermal

evaporation [35] and vapor phase transport [36]. Chemical methods employed include hydrothermal [37], solvothermal [38] and sol-gel [39] methods. While physical methods have been widely used to synthesis one dimensional ZnO nanowires/ nanorods onto various substrates, chemical synthesis methods have gained importance as the synthesis process and conditions are simple, mild and easily scalable for large scale industrial applications. It has been reported earlier that shape and size of the photocatalysts strongly affect their photocatalytic degradation efficiency. Li *et al.* [40] have synthesized ZnO powders with different morphologies by alkali precipitation, organo-zinc hydrolysis, spray pyrolysis and showed that the morphology of particles significantly affects their photocatalytic efficiency. Xu *et al.* [23] synthesized ZnO with different morphology by Solvothermal method and showed that photocatalytic activity is affected by the morphology of nanostructures. Since morphology and size are the crucial factors which determine the photocatalytic efficiency, efforts are being made for size- and shape-controlled synthesis of ZnO nanostructures by facile wet chemical routes. Various factors such as temperature, concentration, capping agent and solvent affect the shape and size of the synthesized ZnO nanostructures [41, 42]. One of the easier ways to control the morphology and size of ZnO nanostructures is by changing the solvent. Khoza *et al.* [3] have prepared ZnO nanostructures with different

morphology by solvothermal method using solvents of different polarities. Xie *et al.* [43] synthesized ZnO whiskers and hexagonal ZnO platelets and studied the effect of solvent on the morphology of synthesized nanostructures. In our earlier works, we have studied the effects of morphology [17], doping [16, 29, 44] and surface modification of ZnO nanostructures on their photocatalytic activities [6, 7, 45]. Ahmad *et al.* [46] have shown that ZnO/graphene composites lead to photocatalytic degradation of methylene blue (MB) dye in 90 minutes. Hu *et al.* [47] have synthesized ZnO nanoparticles using 2-propanol as a solvent. However, they have not studied the photocatalytic activity of the synthesized ZnO nanostructures. Zyoud *et al.* [48] demonstrated the photocatalytic degradation of methyl orange (MO) dye by ZnO nanoparticles.

In this paper, we have synthesized ZnO nanostructures by a facile wet chemical method using different solvents (water, ethanol and propanol) and studied the effects of solvents on the structural, optical and photocatalytic properties of synthesized ZnO nanostructures. The photocatalytic activities of the synthesized ZnO nanostructures were evaluated by studying sunlight driven photocatalytic degradation of methylene blue (MB) and methyl orange (MO) dyes in water. We have demonstrated that ZnO nanostructures prepared by using propanol as solvent exhibit highly enhanced photocatalytic activity for degradation of MB and MO dyes in water. Even though there are studies on photocatalytic activity of ZnO nanostructures, the effects of the solvent on the photocatalytic activity of the synthesized ZnO nanostructures have not been well studied and such high photocatalytic activity observed in the present study has not been achieved. In the present study, we have demonstrated that ZnO nanostructures with highly enhanced photocatalytic activity for degradation of MB and MO dyes in water can be prepared by simply changing the solvent to propanol.

Experimental

Materials

Zinc acetate dihydrate ($\text{Zn}(\text{CH}_3\text{COO})_2 \cdot 2\text{H}_2\text{O}$), potassium hydroxide (KOH), ethanol, propanol, methylene blue (MB) and methyl orange (MO) were purchased from SRL, India. All chemicals used were of analytical grade and were used as received without any further purification.

Synthesis of ZnO nanostructures

For the synthesis of ZnO nanostructures, 0.05 M solutions of zinc acetate dihydrate were prepared in 100 mL double distilled water, ethanol and propanol. These solutions were kept under constant stirring at 60 °C. A calculated amount of KOH with concentration 10 times higher than that of the Zn^{2+} concentration was added into these solutions under rigorous stirring. The solution was stirred for 3 h with the temperature maintained at 60 °C. The solution was then left undisturbed and allowed to cool down over night. The white precipitates formed were obtained by centrifugation and repeatedly washed with double distilled water followed by drying in an oven at 80 °C over night. The solid white powder obtained was used for further characterization and

photocatalytic studies. The schematic diagram of the synthesis method is shown in Fig. 1(a).

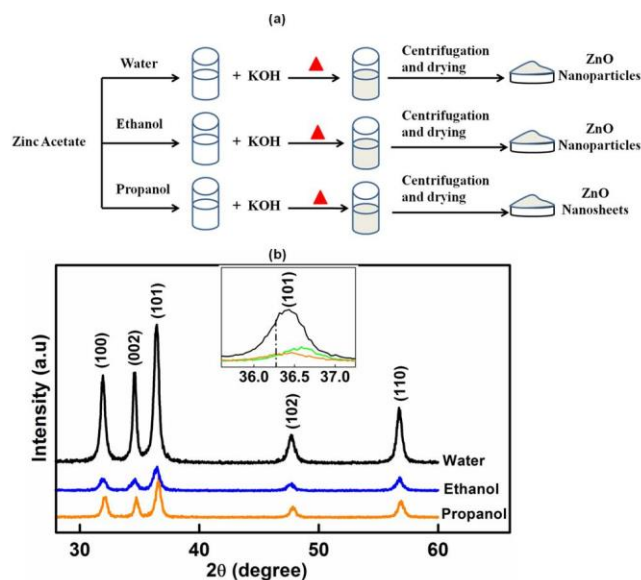


Fig. 1. (a) Schematic diagram showing the synthesis of ZnO nanostructures and (b) XRD patterns of as-synthesized nanostructured ZnO samples. Inset shows the shift in the (101) peak position of all the samples with respect to the bulk value, marked by a dashed-dotted line.

Characterizations

To determine the structural properties powder X-ray diffraction (XRD) studies were carried out at room temperature using a Panalytical X'pert Pro diffractometer with $\text{Cu K}\alpha$ radiation ($\lambda = 0.1542 \text{ nm}$). Field emission scanning electron microscopy (FESEM) was used to study the surface morphology of as-synthesized nanomaterials. The optical properties of the samples were studied by UV-visible absorption spectroscopy using HITACHI U-3300 double beam spectrophotometer. For this the powder samples were dispersed in double distilled water as the reference medium. Raman spectra were recorded using a Horiba Jobin Yvon LabRAM using argon laser (488 nm) with spot size of 1 μm . TEM analysis was carried out using FEI, TF30, S-Twin field emission gun based microscope operating at 300 kV. The TEM facility is equipped with a high-angle annular dark field (HAADF) detector from Fischione (Model 3000) and an energy dispersive X-ray spectroscopy (EDS, EDAX Inc.) attachment.

Photocatalytic measurements

The photocatalytic activities of the as-synthesized ZnO nanostructures were studied by sunlight driven degradation of methylene blue (MB) and methyl orange (MO) dyes in water. For these studies, 5 mg of ZnO nanostructures were ultrasonically dispersed in 5 mL double distilled water in different glass vials. A dye solution was added to reach 10 μM concentration and was thoroughly mixed with the prepared photocatalyst and stirred in dark for 30 minutes to reach adsorption-desorption equilibrium. These solutions containing the dyes and different photocatalysts were exposed to sunlight for different durations of 10, 15 and 20

minutes with intermittent shaking for uniform mixing. The experiments were carried out at mid-day during summer to ensure irradiation with sun light of maximum luminosity. Subsequently, the photocatalysts were removed from these solutions by centrifugation. The concentration of dye in these solutions was monitored by UV-visible absorption spectroscopy in the wavelength range of 200 - 800 nm with double distilled water as the reference medium. To check the reusability of the photocatalyst, repetitive tests were also conducted for three runs. The photocatalytic efficiency of a photocatalyst for degradation of dye was determined by using the following formula;

$$\eta = (C_0 - C)/C_0 \quad (1)$$

where, C_0 is the concentration of dye before addition of any photocatalyst and C is the concentration of dye in the reaction suspension with photocatalyst following sun light irradiation for time t .

Results and discussion

Morphology and crystal structure

Fig. 1(b) shows the XRD patterns of as-synthesized ZnO nanostructure samples. The observed peaks in the spectra can be well indexed to the hexagonal wurtzite structure of crystalline ZnO [JCPDS no. 36-1451]. No extra peaks related to any impurity were observed within the detection limit of the instrument, which confirm that the as-synthesized products are pure. The inset in **Fig. 1** shows the shift in the (101) peak position from the bulk value in case of all the samples. The average crystallite sizes of nanostructures are estimated to be 14.1 nm, 9.9 nm and 12.6 nm for water, ethanol and propanol, respectively. The micro-strain in the ZnO nanostructures was analyzed using Williamson–Hall method given as

$$\frac{\beta \cos(\theta)}{\lambda} = \frac{1}{D_{hkl}} + \varepsilon_{hkl} \frac{\sin(\theta)}{\lambda} \quad (2)$$

where, θ is the diffraction angle, β is the full width at half maxima (FWHM) of XRD peak, λ is the wavelength of the X-rays, D_{hkl} is the effective crystallite size and ε_{hkl} is the micro-strain. The strain in ZnO nanostructures for the samples prepared using water, ethanol and propanol as solvents are estimated to be 0.0017, -0.00048 and 0.0013, respectively.

Fig. 2(a, b) shows the low magnification TEM images of nanostructured ZnO samples, prepared using ethanol and propanol as solvent. It can be clearly seen that both the samples consist of ZnO nanostructures. In the case of sample prepared using propanol, there is presence of nanosheets-like structures formed by oriented attachment of ZnO nanoparticles along with ZnO nanoparticles. These nanosheets-like structures help in enhanced adsorption of dyes due to their higher surface area. **Fig. (c, d)** shows the corresponding HRTEM images of ZnO nanostructures which further clarify the structure. The HRTEM images shows the lattice fringes with spacing of 2.4 Å corresponding to (101) inter-planar spacing of wurtzite ZnO in all the cases. FESEM images of the as-synthesized ZnO samples are shown in **Fig. 2(e-g)**. The average width

and length of the synthesized ZnO nanoparticles are found to be 68.2 nm and 84.6 nm respectively for water, 25.3 nm and 30 nm for ethanol, 33.4 nm and 40.3 nm for propanol. The aspect ratios of ZnO nanostructures for the samples prepared using water, ethanol and propanol as solvent are found to be 1.3, 1.2 and 1.2, respectively. In addition to ZnO nanoparticles, elongated nanostructures formed by oriented attachment of ZnO nanoparticles can be clearly seen in the sample prepared using propanol as the solvent.

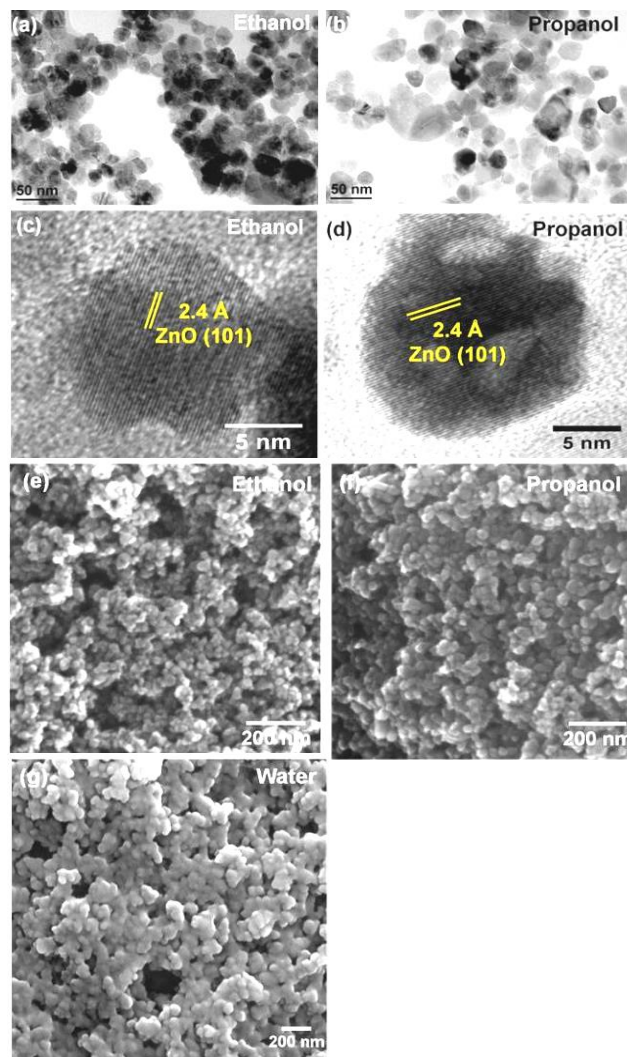


Fig. 2. (a-b) Low magnification TEM images of ZnO nanostructure samples prepared using ethanol and propanol as solvent. (c-d) HRTEM images of ZnO nanostructures in samples prepared using ethanol and propanol showing the lattice fringes. (e-g) FESEM images of ZnO nanostructures in samples prepared using (e) ethanol, (f) propanol and (g) water as solvent.

Optical properties

UV-visible absorption spectra of nanostructured ZnO samples are shown in **Fig. 3(a)**. All the samples show the characteristic excitonic absorption peak of ZnO in the UV region. The band gaps calculated using Tauc plots are estimated to be 3.4 eV, 3.14 eV and 3.14 eV for samples prepared using water, ethanol and propanol, respectively. **Fig. 3(b)** shows the Raman spectra of nanostructured ZnO samples. The strongest peak observed at 435 cm^{-1} is the characteristic $E_2^{(\text{high})}$ peak for ZnO and is associated with

vibration of the oxygen atoms. The peak at 574.1 cm^{-1} is due to $A_1(\text{low})/E_1(\text{low})$ mode. The peaks at 388 cm^{-1} and 409 cm^{-1} correspond to $A_1(\text{TO})$ and $E_1(\text{TO})$ modes, which are the first order optical modes of ZnO. The peak at 537 cm^{-1} is due to 2LA mode which is a second order feature due to multi-phonon process [49]. The intensity of $E_2(\text{high})$ and $A_1(\text{low})/E_1(\text{low})$ peak is higher in case of ZnO prepared using propanol as compared to other samples. The observed enhancement indicates the increased crystallinity of the sample prepared in propanol.

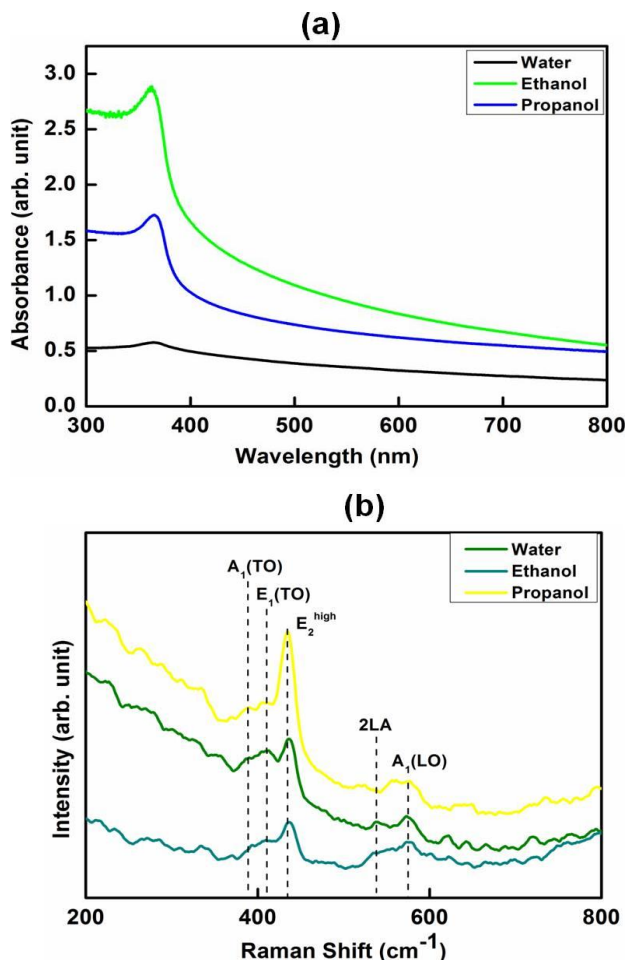


Fig. 3 (a) UV-visible absorption spectra of nanostructured ZnO samples prepared using different solvents. (b) Raman spectra of the nanostructured ZnO samples.

Photocatalytic studies

Fig. 4(a-c) and **Fig. 5(a-c)** show the absorption spectra of $10\ \mu\text{M}$ MB and $10\ \mu\text{M}$ MO dye solutions, respectively with different photocatalysts under sunlight irradiation for different durations of time. The characteristic absorption peaks of MB at 664 nm and MO at 464 nm are monitored for different sun light exposure time. The absorption spectra clearly show that the characteristic absorption peaks diminish in intensity with increase in irradiation time and almost completely disappears after 20 minutes of irradiation. It is observed that ZnO nanostructures prepared using propanol as solvent exhibit the highest photocatalytic efficiency for photocatalytic degradation of both MB and MO dyes in water. The kinetics of photocatalytic degradation for all the photocatalysts are given in **Fig. 4(d)**

and **Fig. 5(d)**, which show the variation of photocatalytic efficiency with sunlight exposure time for different photocatalysts for the degradation of MB and MO dyes in water, respectively. To check the reusability of the photocatalyst, repetition tests were conducted for three runs using ZnO nanostructures prepared in propanol as the photocatalyst. The results of repetitive photocatalytic degradation studies on MB and MO are shown in **Fig. 4(e)** and **Fig. 5(e)**, respectively. In all the runs the nanostructured ZnO photocatalysts showed excellent degradation efficiency, demonstrating its reusability and stability for practical applications.

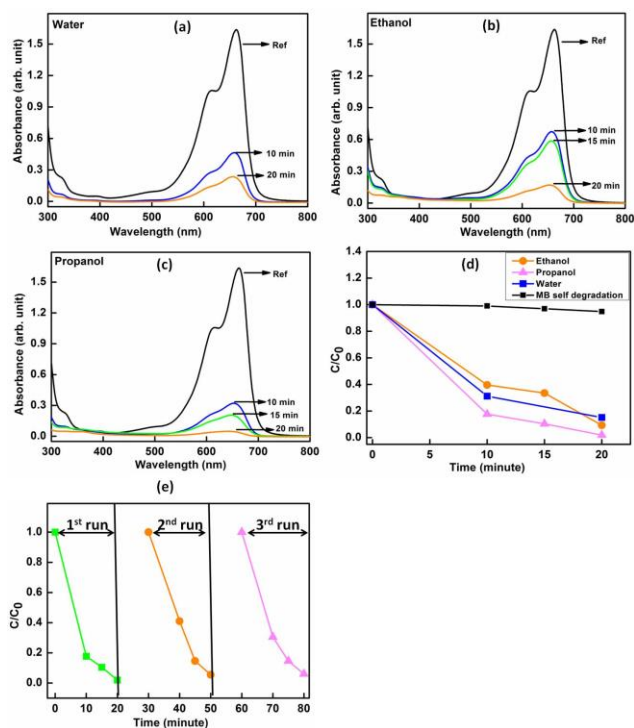
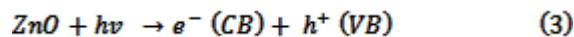


Fig. 4. (a-c) UV-visible absorption spectra showing temporal evolution of photocatalytic degradation of MB upon sun light irradiation using nanostructured ZnO samples as photocatalysts, (d) Variation of photocatalytic efficiency with sunlight exposure time for different photocatalysts and (e) Repetitive tests on nanostructured ZnO sample prepared using propanol for three runs of photocatalytic degradation of MB dye in water.

When ZnO nanostructures with dye molecules adsorbed on their surface are exposed to sunlight, electron and hole pairs are generated in the conduction and valence band of ZnO, respectively. The electrons in the conduction band forms superoxide anion radicals ($\cdot\text{O}_2^-$) by interacting with oxygen molecules while the holes in the valence band interact with surface hydroxyl groups to produce hydroxyl radicals ($\cdot\text{OH}$). Hydroxyl radicals can also be formed by the dissociation of water by the holes in the valence band of ZnO. These highly reactive radicals react with the adsorbed organic dye molecules and leads to their degradation and mineralization. The equations summarizing the above processes [50] are given below and are schematically illustrated in **Fig. 6**.



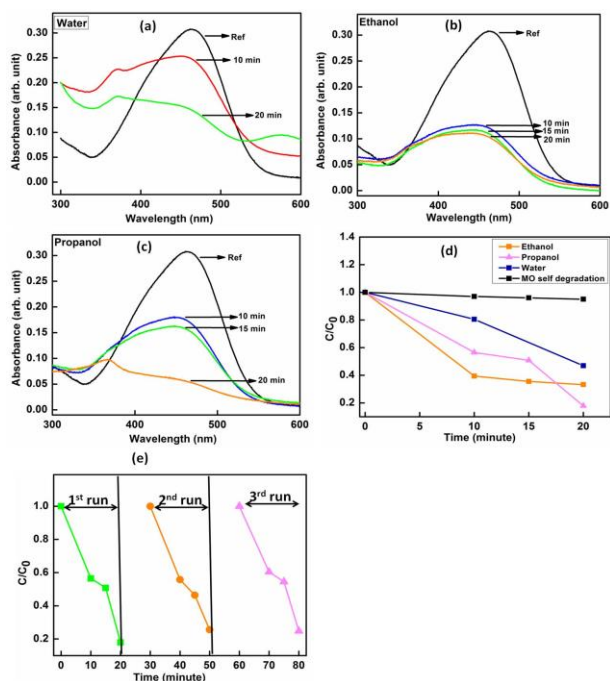
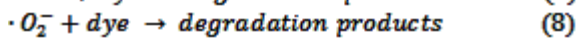
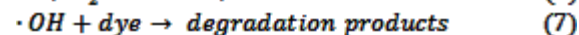
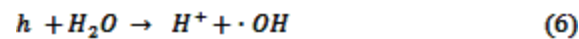


Fig. 5. (a-c). UV-visible absorption spectra showing temporal evolution of photocatalytic degradation of MO upon sun light irradiation using ZnO nanostructure samples as photocatalysts, (d). Variation of photocatalytic efficiency with sunlight exposure time for different photocatalysts. (e) Repetitive tests for nanostructured ZnO sample prepared using propanol for three runs of photocatalytic degradation of MO dye in water.

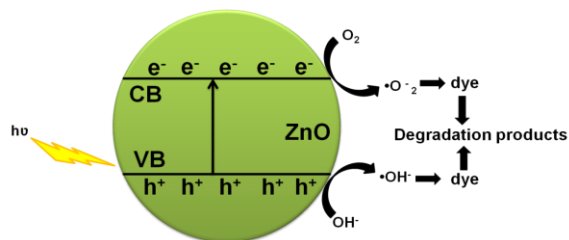


Fig. 6. Schematic band diagram showing the charge transportation processes in nanostructured ZnO photocatalyst leading to the photocatalytic degradation of dye.

The effects of solvent on the morphology of ZnO nanostructures can be understood as follows. The interactions between the solvent and the ZnO nanocrystals during the wet chemical synthesis control the morphology of the nanostructures. The properties of the solvent such as molecular structure, viscosity, vapor pressure affect the formation and growth of ZnO nanostructures [51].

Table 1 shows the values of viscosity of solvents used and the resulting size, lattice strain and photocatalytic efficiency of synthesized ZnO nanostructures.

Table 1. Effect of solvent on photocatalytic efficiency of ZnO nanostructures.

Solvent	Viscosity (mPas)	Crystallite size (nm)	Strain	c/a	Photocatalytic efficiency (%)	
					MB	MO
Water	0.467	14.1	0.0017	1.521	85	53.1
Ethanol	0.57	9.9	-0.00048	1.521	90.7	66.8
Propanol	0.755	12.6	0.0013	1.52	98.1	82.1

The rate of growth in a particular direction differs in different solvents with different polarities. Factors such as initial nucleation of the nanocrystal and the solubility of the precursors in the solvent decide the final morphology of the nanostructures [52]. In our study we have taken three solvents of decreasing polarity: water, ethanol, and propanol. Solvent with high polarity interacts strongly with the polar surface of ZnO, thus reduces the adsorption of growth molecules to the polar surfaces of ZnO [53]. Water having the highest polarity thus produces spherical particles and as the polarity decreases, the formation of anisotropic structures starts. In our case also, water mediated growth shows the presence of spherical nanoparticles and as the polarity decreases, nanosheets like structures form along with spherical nanoparticles. It can be seen that maximum efficiency is observed for propanol mediated growth of ZnO nanostructures. In the case of propanol mediated growth, nanostructures in the form of nanoparticles and nanosheets could be observed. Nanosheets provide higher surface area for adsorption of dye molecules, which leads to higher photocatalytic efficiency for degradation of dyes as observed in the case of ZnO nanostructures prepared using propanol. In our earlier study [16] we had reported that nanodisk like structure shows excellent photocatalytic degradation of organic dyes due to enhanced adsorption of dyes. In general, nanostructures having large surface area can provide larger number of active sites for adsorption of dye molecules as compared to spherical nanoparticles and in turn lead to efficient photocatalytic degradation of dye in water. Zeng *et al.* [54] synthesized ZnO nanodisks and nanowires and showed that photocatalytic activity for photodegradation of Rhodamine B dye was better for ZnO nanodisks with a high population of (0001) facets as compared to ZnO nanowires. Zhai *et al.* [55] synthesized ZnO nanodisks which have high photocatalytic efficiency towards degradation of MO. In our case, ZnO nanosheets formed by propanol mediated growth shows enhanced photocatalytic activities towards degradation of MB and MO dyes as compared to the other samples. It must be pointed out here that the smaller value of lattice strain in the ZnO nanostructures prepared using propanol also contributes to the enhancement in the photocatalytic activity. We attribute the enhanced photocatalytic activity of ZnO nanostructures prepared using propanol as solvent to the higher surface area of ZnO nanosheets which lead to enhanced adsorption of dye molecules and efficient catalytic activity of exposed facets leading to efficient sunlight driven photocatalytic degradation of MB and MO dyes in water.

Conclusion

In summary, we have synthesized ZnO nanostructures by a facile wet chemical method and studied the effects of solvents on the structural, optical and photocatalytic properties of ZnO nanostructures. ZnO nanostructures prepared using propanol exhibited highly enhanced photocatalytic efficiency, leading to almost complete photocatalytic degradation 10 μ M of MB and 10 μ M of MO dyes in only 20 minutes under sun light irradiation. We have demonstrated that propanol mediated growth leads to formation of ZnO nanosheet-like structures formed by oriented attachment of ZnO nanoparticles. We attribute the

highly enhanced photocatalytic activity of ZnO nanostructures prepared in propanol to the high surface area of nanosheet-like structures formed, which lead to enhanced adsorption of dye molecules resulting in efficient photocatalytic degradation of dyes upon sunlight irradiation.

Acknowledgements

The authors are thankful to Prof. S. Annapoorni and Prof. Vinay Gupta for extending facilities for PL and Raman studies, Dr. Saif A. Khan and Srikanth for their help in FESEM and XRD measurements, respectively. SM is thankful to University Grants Commission (UGC), New Delhi for funding under Major Research Project (F. No: 41-865/2012 (SR)). SM is thankful to Department of Science and Technology (DST), New Delhi for providing XRD facility under Nano Mission program. SK is thankful to Guru Gobind Singh Indraprastha University, New Delhi for providing financial assistance through IP Fellowship.

Author contributions

Conceived the plan: SM; Performed the experiments:SK, BS, SM; Data analysis: SK; Wrote the paper: SK, SM (SK, BS, SM are the initials of authors). Authors have no competing financial interests.

Reference

- Tian, C.; Zhang, Q.; Wu, A.; Jiang, M.; Liang, Z.; Jiang, B.; Fu, H. *Chem. Comm.* **2012**, *48*, 2858.
DOI: [10.1039/c2cc16434e](https://doi.org/10.1039/c2cc16434e)
- Talebian, N.; Amininezhad, S. M.; Doudi, M. *J. Photochem. Photobiol. B* **2013**, *120*, 66.
DOI: [10.1016/j.jphotochem.2013.01.004](https://doi.org/10.1016/j.jphotochem.2013.01.004)
- Sikora, B.; Fronc, K.; Kaminska, I.; Korczyk, A. B.; Sobczak, K.; Dłużewski, P.; Elbaum, D. *J. Sol-Gel Sci. Technol.* **2012**, *61*, 197.
DOI: [10.1007/s10971-011-2614-5](https://doi.org/10.1007/s10971-011-2614-5)
- Cheng, B.; Samulski, T. *Chem. Commun.* **2004**, 986–987.
DOI: [10.1039/B316435G](https://doi.org/10.1039/B316435G)
- Hong, R. Y.; Li, J. H.; Chen, L. L.; Liu, D. Q.; Li, H. Z.; Zheng, Y.; Ding, J. *Powder Technol.* **2009**, *189*, 426.
DOI: [10.1016/j.powtec.2008.07.004](https://doi.org/10.1016/j.powtec.2008.07.004)
- Kuriakose, S.; Choudhary, V.; Satpati, B.; Mohapatra, S. *Phys. Chem. Chem. Phys.* **2014**, *16*, 17560.
DOI: [10.1039/c4cp02222a](https://doi.org/10.1039/c4cp02222a)
- Kuriakose, S.; Choudhary, V.; Satpati, B.; Mohapatra, S. *Beilstein J. Nanotechnol.* **2014**, *5*, 639.
DOI: [10.3762/bjnano.5.75](https://doi.org/10.3762/bjnano.5.75)
- Dong, H.; Liu, Y.; Lu, J.; Chen, Z.; Wang, J.; Zhang, L. *J. Mater. Chem. C* **2013**, *1*, 202.
DOI: [10.1039/C2TC00070A](https://doi.org/10.1039/C2TC00070A)
- Park, Y. K.; Choi, H. S.; Kim, J. H.; Kim, J. H.; Hahn, Y. B. *Nanotechnology* **2011**, *22*, 185310.
DOI: [10.1088/0957-4484/22/18/185310](https://doi.org/10.1088/0957-4484/22/18/185310)
- Khurana, G.; Sahoo, S.; Barik, S. K.; Katiyar, R. S. *J. Alloys Compd.* **2013**, *578*, 257.
DOI: [10.1016/j.jallcom.2013.05.080](https://doi.org/10.1016/j.jallcom.2013.05.080)
- Seow, L. S.; Wong, A. S. W.; Thavasi, V.; Jose, R.; Ramakrishna, S.; Ho, G. W. *Nanotechnology* **2009**, *20*, 045604.
DOI: [10.1088/0957-4484/20/4/045604](https://doi.org/10.1088/0957-4484/20/4/045604)
- Xu, H.; Liu, X.; Cui, D.; Li, M.; Jiang, M. *Sens. Actuators B* **2006**, *114*, 301.
DOI: [10.1016/j.snb.2005.05.020](https://doi.org/10.1016/j.snb.2005.05.020)
- Tian, Z. R.; Voigt, J. A.; Liu, J.; Mckenzie, B.; Mcdermott, M. J.; Rodriguez, M. A.; Konishi, H.; Xu, H. *Nat. Mater.* **2003**, *2*, 821.
DOI: [10.1038/nmat1014](https://doi.org/10.1038/nmat1014)
- Yassitepe, E.; Yatmaz, H. C.; Ozturk, C.; Ozturk, K.; Duran, C. *J. Photochem. Photobiol. A* **2008**, *198*, 1.
DOI: [10.1016/j.jphotochem.2008.02.007](https://doi.org/10.1016/j.jphotochem.2008.02.007)
- Wang, X.; Zhang, Q.; Wan, Q.; Dai, G.; Zhou, C.; Zou, B. *J. Phys. Chem. C* **2011**, *115*, 2769.
DOI: [10.1021/jp1096822](https://doi.org/10.1021/jp1096822)
- Kuriakose, S.; Satpati, B.; Mohapatra, S. *Phys. Chem. Chem. Phys.* **2014**, *16*, 12741.
DOI: [10.1039/C4CP01315H](https://doi.org/10.1039/C4CP01315H)
- Kuriakose, S.; Bhardwaj, N.; Singh, J.; Satpati, B.; Mohapatra, S. *Beilstein J. Nanotechnol.* **2013**, *4*, 763.
DOI: [10.3762/bjnano.4.87](https://doi.org/10.3762/bjnano.4.87)
- Liqiang, J.; Yichun, Q.; Baiqi, W.; Shudan, L.; Baojiang, J.; Libin, Y.; Wei, F.; Honggang, F.; Jiazhong, S. *Sol. Energy Mat. Sol. Cells* **2006**, *90*, 1773.
DOI: [10.1016/j.solmat.2005.11.007](https://doi.org/10.1016/j.solmat.2005.11.007)
- Zeng, H.; Cai, W.; Liu, P.; Xu, X.; Zhou, H.; Klingshirn, C.; Kalt, H. *ACS Nano* **2008**, *2*, 1661.
DOI: [10.1021/nm800353q](https://doi.org/10.1021/nm800353q)
- Mclaren, A.; Solis, T. V.; Li, G.; Tsang, S. C. *J. Am. Chem. Soc.* **2009**, *131*, 12540.
DOI: [10.1021/ja9052703](https://doi.org/10.1021/ja9052703)
- Reimer, T.; Paulowicz, I.; Röder, R.; Kaps, S.; Lupan, O.; Chemnitz, S.; Benecke, W.; Ronning, C.; Adelung, R.; Mishra, Y. K. *ACS Appl. Mater. Interfaces* **2014**, *6*, 7806.
DOI: [10.1021/am5010877](https://doi.org/10.1021/am5010877)
- Mishra, Y. K.; Modi, G.; Cretu, V.; Postica, V.; Lupan, O.; Reimer, T.; Paulowicz, I.; Hrkac, V.; Benecke, W.; Kienle, L.; Adelung, R. *ACS Appl. Mater. Interfaces* **2015**, *7*, 14303.
DOI: [10.1021/acsami.5b02816](https://doi.org/10.1021/acsami.5b02816)
- Xu, L.; Hu, Y. L.; Pelligra, C.; Chen, C. H.; Jin, L.; Huang, H.; Sithambaram, S.; Aindow, M.; Joesten, R.; Suib, S. L. *Chem. Mater.* **2009**, *21*, 2875.
DOI: [10.1021/cm900608d](https://doi.org/10.1021/cm900608d)
- Antoine, T.; Mishra, Y. K.; Trigilio, J.; Tiwari, V.; Adelung, R.; Shukla, D. *Antiviral Res.* **2012**, *96*, 363.
DOI: [10.1016/j.antiviral.2012.09.020](https://doi.org/10.1016/j.antiviral.2012.09.020)
- Papavlassopoulos, H.; Mishra, Y. K.; Kaps, S.; Paulowicz, I.; Abdelaziz, R.; Elbahri, M.; Maser, E.; Adelung, R.; Röhl, C. *PLoS ONE* **2014**, *9*, e84983.
DOI: [10.1371/journal.pone.0084983](https://doi.org/10.1371/journal.pone.0084983)
- Mishra, Y. K.; Kaps, S.; Schuchardt, A.; Paulowicz, I.; Jin, X.; Gedamu, D.; Freitag, S.; Claus, M.; Wille, S.; Kovalev, A.; Gorb, S. N.; Adelung, R. *Particle Particle Systems Character.* **2013**, *30*, 775.
DOI: [10.1002/ppsc.201300197](https://doi.org/10.1002/ppsc.201300197)
- Jin, X.; Götz, M.; Wille, S.; Mishra, Y. K.; Adelung, R.; Zollfrank, C. *Adv. Mater.* **2013**, *25*, 1342.
DOI: [10.1002/adma.201203849](https://doi.org/10.1002/adma.201203849)
- Gedamu, D.; Paulowicz, I.; Kaps, S.; Lupan, O.; Wille, S.; Haidarschin, G.; Mishra, Y. K.; Adelung, R. *Adv. Mater.* **2014**, *26*, 1541.
DOI: [10.1002/adma.201304363](https://doi.org/10.1002/adma.201304363)
- Kuriakose, S.; Satpati, B.; Mohapatra, S., *Phys. Chem. Chem. Phys.*, **2015**, *17*, 25172.
DOI: [10.1039/C5CP01681A](https://doi.org/10.1039/C5CP01681A)
- Chou, S. M.; Teoh, L. G.; Lai, W. H.; Su, Y. H.; Hon, M. H. *Sensors* **2006**, *6*, 1420.
DOI: [10.3390/s6101420](https://doi.org/10.3390/s6101420)
- Zheng, Z. Q.; Yao, J. D.; Wang, B.; Yang, G. W. *Sci. Reports* **2015**, *5*, 11070.
DOI: [10.1038/srep11070](https://doi.org/10.1038/srep11070)
- Orsini, A.; Falconi, C. *Sci. Reports* **2014**, *4*, 6285.
DOI: [10.1038/srep06285](https://doi.org/10.1038/srep06285)
- Shafiei, S.; Nourbakhsh, A.; Ganjipour, B.; Zahedifar, M.; Nezhad, G. V. *Nanotechnology* **2007**, *18*, 355708.
DOI: [10.1088/0957-4484/18/35/355708](https://doi.org/10.1088/0957-4484/18/35/355708)
- Kong, Y. C.; Yu, D. P.; Zhang, B.; Fang, W.; Feng, S. Q. *Appl. Phys. Lett.* **2001**, *78*, 407.
DOI: [10.1063/1.1342050](https://doi.org/10.1063/1.1342050)
- Yao, B. D.; Chan, Y. F.; Wang, N. *Appl. Phys. Lett.* **2002**, *81*, 757.
DOI: [10.1063/1.1495878](https://doi.org/10.1063/1.1495878)
- Park, W. I.; Kim, D. H.; Jung, S. W.; Yi, G. C. *Appl. Phys. Lett.* **2002**, *80*, 4232.
DOI: [10.1063/1.1482800](https://doi.org/10.1063/1.1482800)
- Pal, U. and Santiago, P. *J. Phys. Chem. B* **2005**, *109*, 15317.
DOI: [10.1021/jp052496i](https://doi.org/10.1021/jp052496i)
- Zhang, A. Q.; Zhang, L.; Sui, L.; Qian, D. J.; Chen, M. *Cryst. Res. Technol.* **2013**, *48*, 947.
DOI: [10.1002/crat.201300143](https://doi.org/10.1002/crat.201300143)
- Tokumoto, M. S.; Pulcinelli, S. H.; Santilli, C. V.; Brioso, V. *J. Phys. Chem. B* **2003**, *107*, 568.
DOI: [10.1021/jp0217381](https://doi.org/10.1021/jp0217381)
- Li, D. and Hamed, H. *Chemosphere* **2003**, *51*, 129.
DOI: [10.1016/S0045-6535\(02\)00787-7](https://doi.org/10.1016/S0045-6535(02)00787-7)
- Jun, Y. W.; Choi, J. S. and Cheon, J. *Angew. Chem. Inter. Ed.* **2006**, *45*, 3414.
DOI: [10.1002/anie.200503821](https://doi.org/10.1002/anie.200503821)
- Tang, C.; Fan, S.; Chapelle, M. L. D. L.; Dang, H.; Li, P. *Adv. Mater.* **2000**, *12*, 1346.

- DOI: [10.1002/1521-4095\(200009\)12:18<1346::AID-ADMA1346>3.0.CO;2-8](https://doi.org/10.1002/1521-4095(200009)12:18<1346::AID-ADMA1346>3.0.CO;2-8)
43. Xie, J.; Li, P.; Li, Y.; Wang, Y.; Wei, Y. *Mater. Lett.* **2008**, *62*, 2814.
DOI: [10.1016/j.matlet.2008.01.053](https://doi.org/10.1016/j.matlet.2008.01.053)
44. Kuriakose, S.; Satpati, B.; Mohapatra, S. *Adv. Mater. Lett.* **2015**, *6*, 217.
DOI: [10.5185/amlett.2015.5693](https://doi.org/10.5185/amlett.2015.5693)
45. Kuriakose, S.; Avasthi, D. K.; Mohapatra, S. *Beilstein J. Nanotechnol.* **2015**, *6*, 928.
DOI: [10.3762/bjnano.6.96](https://doi.org/10.3762/bjnano.6.96)
46. Ahmad, M.; Ahmed, E.; Hong, Z.L.; Xu, J. F.; Khalid, N. R.; Elhissi, A.; Ahmed, W. *Appl. Surf. Sci.* **2013**, *274*, 273.
DOI: [10.1016/j.apsusc.2013.03.035](https://doi.org/10.1016/j.apsusc.2013.03.035)
47. Hu, Z.; Ramírez, D. J. E.; Cervera, B. E. H.; Oskam, G.; Searson, P. C. *J. Phys. Chem. B* **2005**, *109*, 11209.
DOI: [10.1021/jp0506033](https://doi.org/10.1021/jp0506033)
48. Zyoud, A.; Zúbi, A.; Helal, M. H. S.; Park, D.; Campet, G.; Hilal, H. *S. J. Environ. Health Sci. Eng.* **2015**, *13*, 46.
DOI: [10.1186/s40201-015-0204-0](https://doi.org/10.1186/s40201-015-0204-0)
49. Zhao, J.; Yan, X.; Yang, Y.; Huang, Y.; Zhang, Y. *Mater. Lett.* **2010**, *64*, 569.
DOI: [10.1016/j.matlet.2009.11.074](https://doi.org/10.1016/j.matlet.2009.11.074)
50. Legrini, O.; Oliveros, E.; Braun, A. M. *Chem. Rev.* **1993**, *93*, 671.
DOI: [10.1021/cr00018a003](https://doi.org/10.1021/cr00018a003)
51. Rezapoura, M.; Talebian, N. *Mater. Chem. Phys.* **2011**, *129*, 249.
DOI: [10.1016/j.matchemphys.2011.04.012](https://doi.org/10.1016/j.matchemphys.2011.04.012)
52. Talebian, N.; Amininezhad, S. M.; Doudi, M. *J. Photochem. Photobiol. B: Bio.* **2013**, *120*, 66.
DOI: [10.1016/j.jphotobiol.2013.01.004](https://doi.org/10.1016/j.jphotobiol.2013.01.004)
53. Xu, S.; Wang, Z. L. *Nano Res.* **2011**, *4*, 1013.
DOI: [10.1007/s12274-011-0160-7](https://doi.org/10.1007/s12274-011-0160-7)
54. Zeng, J. H.; Jin, B. B.; Wang, Y. F.; *Chem. Phys. Lett.*, **2009**, *472*, 90.
DOI: [10.1016/j.cplett.2009.02.082](https://doi.org/10.1016/j.cplett.2009.02.082)
55. Zhai, T.; Xie, S.; Zhao, Y.; Sun, X.; Lu, X.; Yu, M.; Xu, M.; Xiao, F.; Tong, Y. *Cryst Eng Comm*, **2012**, *14*, 1850.
DOI: [10.1039/C1CE06013A](https://doi.org/10.1039/C1CE06013A)

Advanced Materials Letters

Copyright © VBRI Press AB, Sweden

www.vbripress.com

Publish your article in this journal

Advanced Materials Letters is an official international journal of International Association of Advanced Materials (IAAM, www.iaamonline.org) published by VBRI Press AB, Sweden monthly. The journal is intended to provide top-quality peer-review articles in the fascinating field of materials science and technology particularly in the area of structure, synthesis and processing, characterisation, advanced-state properties, and application of materials. All published articles are indexed in various databases and are available download for free. The manuscript management system is completely electronic and has fast and fair peer-review process. The journal includes review article, research article, notes, letter to editor and short communications.

